Use of Data Surface Models (DSM) derived from UAV images to estimate water depths for four undisturbed coastal marshes of eastern Georgian Bay

By:

*Dr. Pat Chow-Fraser**
and
Sherry Chen, B.Sc.

McMaster University,
Department of Biology
1280 Main Street West, Hamilton,
ON L8S 4K1, Canada

Submitted to:
Dr. James Marcaccio,
Post-doctoral fellow
GLLFAS, Fisheries and Oceans Canada,
867 Lakeshore Rd., Burlington,
ON L7S 1A1, Canada

March 29, 2021

*Corresponding email: chowfras@mcmaster.ca

INTRODUCTION

Background

Unmanned aerial vehicles (UAVs) or drones can be used as an effective mapping tool in terrestrial and semi-aquatic environments. Drones provide extremely high-resolution image data that are timely for the project in question. With advanced software, the image data collected can be transformed into continuous two-dimensional maps with an additional three-dimensional data layer providing surface and bare earth models (digital surface models (DSMs) and digital elevation models (DEMs), respectively). Height derived from these three-dimensional data layers (i.e., elevation) has been shown to be accurate over terrestrial areas, although the elevation or resolution of the height data is somewhat lower than that of the two-dimensional data (often 3 times the two-dimensional resolution or greater). Available research to date has not described the potential or effectiveness of these elevation data for aquatic environments (i.e., deriving bathymetry) or how light transmission through the water column may alter the results. Light travels at different velocities when travelling through water, and the transition from air to water and back to air may alter the perceived depth by drone software.

Objective of study

The objective of this contract is to determine if DSM derived from drone images taken over vegetated wetlands in Georgian Bay can yield accurate depth information compared with those obtained by sonar, and to determine whether correction factors accounting for environmental differences among sites could be used to increase accuracy.

Approach

An explicit condition for this project is that we use only existing data, including those that had not necessarily been collected with the goal of this project in mind. Therefore, the first step was to conduct an exhaustive search through existing drone images and bathymetric datasets to determine how many wetlands would be suitable for inclusion within the time frame of this project. We selected four wetlands: North Bay 1, Venning's Bay, Ojibway Bay and Green Island (see **Figure 1**). Details on when UAV images and DEM data were acquired are presented in **Table 1**. Except for Ojibway Bay, UAV images for the three other wetlands had been acquired twice between 2015 and 2017. Bathymetric information acquired by sonar were also available to build DEMs for each of these wetlands.

1. The first task was to assess the accuracy of drone-based 3-dimensional data against dGPS data to confirm the utility of the DSM for terrestrial environments.
2. We then compared depths derived from DSM and DEM for the four wetlands to determine the accuracy of drone-based data for wetland environments (see Table 1 for information on the dates of sampling). As part of this task, we examined the effect of different habitat classes or spatial features on depth estimates. Based on this assessment, we excluded some classes/features that had great disparities between DSM and DEM estimates.

3. We determined a correction factor that could be applied to generate DEM from DSM and evaluated how these data can be integrated with elevation models for terrestrial scenes.
4. We determined limitations of this approach to estimating depths for heavily vegetated environments and will make recommendations on how to proceed in future studies.

Literature Review

Bathymetric data are useful for studying flood management, understanding flow direction, and ecosystem management. They are valuable but often difficult to acquire compared with terrestrial elevation data. Bathymetric surveys typically rely on use of sonar technology to collect depth readings based on sound saves bouncing off substrate (Pillay et al., 2020). The sonar transducer must be mounted on a boat and there are minimum and maximum depth limits depending on the particular device model. Sonar technology requires the transducer emitting sound to be mounted on a vessel (boat, canoe or remotely operated vehicle), and for this vessel to travel throughout the water body. In heavily vegetated wetlands such as those in Georgian Bay, operating a boat through shallow depths can be challenging, and thus depths lower than 0.75 m are generally unreliable. There are alternatives to use of sonar technology, including use of bathymetric LiDAR that can penetrate water using green light rather than near infrared light commonly used for terrestrial systems (USDC, 2012). LiDAR acquired depths are the gold standard, which can have an accuracy of ±2.5 cm at depths less than 5 meters, and ±10 cm at depths beyond 5 meters up to 40 meters (Paul et al., 2020). Unfortunately, LiDAR technology is expensive and not within reach of most research budgets. Another option is to use infrared sensors above the water to penetrate shallow depths. Previous studies that used this in aquatic ecosystems showed that accuracy was dependent on temperature and salinity (Pegau et al., 1997), making them less reliable than LiDAR or sonar.

UAVs are commonly used to map terrestrial vegetation, but few studies were found for bathymetry modelling in water. A study carried out in a temperate fluvial environment found that UAV-derived DSM/DEM were more accurate than the RTK-dGPS data when compared with LiDAR measurements (Mazzoleni et al., 2020). The range of depth data for this river system was about 20 m, and there was limited vegetation in/on the water. Therefore, use of UAV-derived DSMs have shown great promise for mapping terrestrial habitats and riverine systems. Fewer studies have focused on the use of DSMs on lentic environments. In a very recent study, Monteiro et al. (2021) used UAV-derived DSMs to determine depth classes (2 meter intervals) of a salt-water wetland, where depths ranged from 1 to 14 m. The wetland was rocky but not densely vegetated and the water was very clear (not highly coloured). To date, no study has compared UAV-derived DSMs against bathymetric information from DEMs derived from sonar boating surveys in freshwater coastal wetlands.

The wetlands in Georgian Bay are relatively shallow (<5 m maximum depth) compared to those in published studies. In addition to the shallow depths, many of the wetlands are dystrophic with high organic content in water that render them tea-stained. This colour could lead to inaccuracies but has not yet been investigated.

METHOD SUMMARY

Multi-rotor image acquisition

The multi-rotor UAV used in this study was a DJI Phantom 2 Vision+ (DJI, Nanshan district, Shenzen, China), operated with a Samsung Galaxy S3 (running Android 4.3 "Jelly Bean") and the DJI Vision application. All details of how the UAV was operated, and the images were stitched together to form mosaics have been described in Marcaccio et al. 2016.

Acquisition of elevations with dGPS

We used a digital GeoXH Global Positioning System (dGPS) according to instructions provided by the manufacturer to collect spot elevation data above the shoreline of the North Bay 1 wetland on August 18, 2016 (see map in **Figure 2a**). There were also some dGPS points for Green Island but because they had been taken during low water levels in 2013, the location of many of these points were below the corresponding shoreline of the drone mosaic that had been acquired in 2016 and 2017.

Sonar acquisition of depth data

We used an off-the-shelf sonar unit (Lowrance HDS7; horizontal accuracy approx. 3 m, vertical accuracy approx. 30 cm) to collect bathymetric data in our wetlands (as per Weller and Chow-Fraser 2019). The data collected were processed into BioBase to convert the SL2 files into point Shapefiles. A manual offset of 0.2 m or 0.1 m was applied to the depth values depending on the vessel used to account for the extra distance of the transducer below the water surface.

Creation of DEMs

Points to create the DEMs came from various sources: readings from a boat-mounted sonar, manually acquired dGPS points, subsidized by a few points acquired by a handheld mobile mapping device, and elevation data from the moderate-resolution DEM created by Weller and Chow-Fraser (2019). We interpolated the assembled points using an ArcGIS tool (Topo to Raster), which produced a bathymetric model that had the lowest RMSE values, and which is based on the ANUDEM program (Arseni et al., 2019). Apart from statistical accuracy, we found the resulting DEM to be visually more accurate than the kriging interpolation method (also associated with low RMSE values compared with IDW or Global Polynomial methods). Parameters of the tool used were: 'Point elevation' as the input feature data type, 'Do not enforce' for the drainage enforcement, and 0.05 as the output surface raster to closely match the DSM resolution of approximately 0.031 m.

Creation of DSMs

The DSM were processed in Pix4Dmapper software. The mosaic drone image and the DSM were georeferenced to the ESRI basemap with projection, NAD83 17N with a vertical projection of NAVD88 (depth). A common problem when georeferencing wetlands is the lack of permanent reference points such as roads or building corners in built-up areas. Although points on rocks can be used as a reference point, the ESRI basemap was often too blurry for this purpose. Corner of docks can be used but this can also lead to inaccuracies because of the wind-induced swaying at the time of image acquisition. We never used the shoreline to perform the georeferencing because water levels on the day of image acquisition seldom matched that of the basemap. Furthermore, it was difficult to distinguish the shoreline from other features because of the low resolution of the basemap. After matching the drone image and DSM to the basemap as best we could, the georeferenced DSM was then rescaled to match the DEM. For example, the range of the DSM values of North Bay 1 was -83 to -31 m. The dGPS data were used as the reference elevation values (see **Figure 2a; Table 2**). The difference between dGPS and DSM were averaged and this value was used in the tool, Raster Calculator, to add to each pixel of the DSM. These steps resulted in a rescaling of the DSM from 157 to 211 m for the North Bay 1 Wetland. As explained earlier, we could not use the Green Island dGPS data due to most of them being below the shoreline of the drone image. The two other wetlands, Venning's Bay and Ojibway Bay did not have dGPS data, and the wetlands that had dGPS data were not sufficiently extensive to cover the entire shoreline. Therefore, all wetlands included the use of land elevation data obtained from Weller and Chow-Fraser's (2019) 10-m resolution DEM. This was very coarse, but we managed to rescale the DSM values so that the zero-meter contour appeared to match the shoreline. With these problems determining the shoreline and rescaling the DSM, we could only use the DSM depth values as a relative measure, so that accuracies associated with the microhabitats/spatial features can be compared across relative depth categories.

Comparing effects of microhabitats/features on accuracies

Despite the high resolution of the drone mosaic, the habitat classes and spatial features themselves could interfere with depth accuracy. These classes included: clear water (CLEAR), floating vegetation (FV), submersed aquatic vegetation (SAV), terrestrial vegetation (TV), rock under water (RUW), rock above water (RAW), glare on water (GLARE), and rendering imperfections (RI) (see samples of these in **Figure 3**; **Appendix Table A1 and 2**); other classes included shadows, waves, and emergent vegetation (not found or considered in **Figure 3**). For example, the glare on top of the water (e.g. example in North Bay 1 in **Figure 2b**), presence of aquatic vegetation, and some discontinuous and erratic data associated with rendering imperfections (e.g. problems associated with the image stitching) could systematically lead to large disparities between DSM and DEM. Since every mosaic had this problem, we decided to conduct a preliminary analysis to see if there were systematic interferences associated with any specific habitat class or spatial feature.

We selected five square quadrats (25 m^2) (see **Figures 3 and 4**) in every class of every mosaic for this comparison. Using the Clip tool, the DSM and DEM were clipped to the feature groups. Afterwards, we used the Raster Calculator to obtain the difference between the DEM and DSM values, and then the Zonal Statistics by Table tool to show the statistics of the derived raster. Statistics calculated included the minimum, maximum, mean and range of differences within each quadrat. To compare among the five quadrats, we calculated an overall mean, an overall range, as well as the range of the quadrat means. This was repeated for all spatial feature types. Since the DSM was not always rescaled to the exact value, we could only make comparisons on a relative basis among feature types. All values were compared as a percentage of the maximum.

Comparing depth estimates from DSM and DEM

To compare accuracies of DSM and DEM, we first created contours from the DEM using the Contour tool, at 0.5 m intervals from the shoreline to a maximum depth of 2.5 m. Eight to ten quadrats (25 m^2) were placed along each contour line. The reason for this range was because a few wetlands were too small to apply 10 quadrats at every depth contour, and therefore, we placed a minimum of 8 quadrats. Unfortunately, the Green Island imagery taken in 2017 was too small for this comparison and had to be excluded from this analysis. After examining the data, we discovered that the accuracy of data at the 0.5 m interval were unacceptable and had to exclude these. Based on results of this task, we were able to avoid areas such as FV and RI, but because of the limited number of images and area available for comparison, we could not avoid using all features that posed problems. The DSM and DEM were clipped to all quadrats and the differences between DSM and DEM within quadrats were determined. Using the Zonal Statistics as Table tool, the mean of all cells was calculated. The values were used to create a linear regression between the DEM and DSM.

Light extinction coefficients

We used a Li-Cor spherical quantum sensor with Li-Cor photometer to collect relative light measurements from just below the water surface down to at least 1.0 m depth at 10-cm intervals. We ensured that all readings taken in a single visit were standardized with respect to meteorological conditions so that readings were consistently in the shade or sunlight. Five replicate readings were taken at each depth and then averaged. We followed the method of Lind (1985) to calculate light extinction coefficients.

RESULTS

Comparing elevation data derived from DSM and dGPS points

We found a highly significant linear relationship between elevation data derived from both techniques (r^2=0.947, P<0.0001; **Figure 5**). The regression coefficient was 0.965 which is very close to 1.00, and the intercept was -0.078 which is also close to the origin.

Comparing depths from DSM and DEM for different microhabitats/features

There were some general trends in discrepancies between DSM and DEM depth estimates across the four wetlands (**Figure 6**). For the North Bay and Venning's Bay images, Terrestrial Vegetation was associated with relatively high discrepancies. This habitat class was not as much of an issue for Green Island because the drone images had been acquired over water for the most part rather than on the land. Discrepancies related to clear water, glare, shadow and waves were noted in all wetlands, although the extent of these discrepancies varied across sites and months. Rendering imperfections were also associated with large discrepancies in all of the wetlands, especially for Ojibway Bay. It is noteworthy that discrepancies for spatial features were conserved within wetlands over different years. It is also interesting to see how aquatic vegetation had very different effects on the Green Island image compared with the Venning's Bay image. We also found reduced discrepancies associated with aquatic vegetation in August compared to June for both the North Bay and Venning's Bay wetlands.

Comparing depth data derived from DSM and DEM

To first inspect the predictive power of DSM, we regressed DEM against DSM for each wetland; this would allow us in the future to derive DEM from DSM. Since we had data from June, July and August, we performed regressions separately for each wetland by month. We found no significant positive relationship for either North Bay and Venning's Bay during August. In fact, there was a significant negative relationship for Venning's Bay that is difficult to explain (**Figure 7**). Therefore, we excluded the August data and performed a regression for only the combined June and July data from all wetlands. We found a highly significant relationship between DEM and DSM but the best-fit line only explained 31% of the variation (**Figure 8a; Eq. 1**).

Eq. 1: DEM = 1.131 + 0.3081*DSM $F(1, 145) = 63.66$, $r^2 = 0.31$, $P<0.0001$, RMSE=0.50

There were some low DSM values from Venning's Bay that appeared to be anomalous, and therefore, we removed these and re-ran the analysis. This reduced the r^2-value slightly, but the slope of the equation increased noticeably, and was closer to the line of unity (**Figure 8b; Eq. 2**).

Eq. 2: DEM = 1.057 + 0.3603*DSM $F(1, 140) = 60.53$, $r^2 = 0.30$, $P<0.0001$, RMSE=0.50

To better understand the relationship between DSM and DEM, we performed the regression with DEM as the predictor. The slope of the regression line was almost 1.00 (**Figure 9a; Eq. 3**), with an intercept of 0.40. This means that on average, the DSM depth estimates were 40 cm lower than corresponding DEM depth measurements.

Eq. 3: DSM = -0.397 + 0.9904*DEM $F(1, 145) = 63.66$, $r^2 = 0.31$, $P<0.0001$, RMSE=0.89

When the low DSM values from Venning's Bay were excluded, we obtained a slightly lower slope (0.84) (**Figure 9b; Eq. 4**), but overall a much better model relating DSM to DEM.

Eq. 4: $DSM = -0.08266 + 0.8377*DEM$ $F(1, 140)= 60.53$, $r^2 = 0.30$, $P<0.0001$, $RMSE=0.76$

When we performed linear regression separately by wetland (using only June and July data), we found a family of lines around the line of unity (**Figure 10; Eq. 5, 6, 7, 8** for Green Island, North Bay 1, Ojibway Bay, and Venning's Bay, respectively).

Eq. 5: $DSM = -0.2859 + 0.5247*DEM$ $F(1, 38)= 10.15$, $r^2 = 0.21$, $P<0.0029$, $RMSE=0.55$

Eq. 6: $DSM = 1.0751 + 0.5234*DEM$ $F(1, 38)= 11.42$, $r^2 = 0.23$, $P<0.0017$, $RMSE=0.54$

Eq. 7: $DSM = 0.6473+0.4125*DEM$ $F(1, 35)= 63.66$, $r^2 = 0.20$, $P<0.0060$, $RMSE=0.46$

Eq. 8: $DSM = -0.1696 + 0.8872*DEM$ $F(1, 23)=5.18$, $r^2 = 0.18$, $P<0.0325$, $RMSE=0.84$

Using ANCOVA, we determined that there were no significant differences among slopes for the wetlands (P=0.2530). Therefore, it was valid for us to directly compare the intercepts among the wetlands. The only significant difference in intercepts was that between North Bay 1 (Eq. 6) and Green Island (Eq. 5).

Archived light extinction data were available for each wetland, but some of these do not correspond to the date when the drone image had been acquired (**Table 1**). Given the small sample size, we used non-parametric Spearman's rank test to determine correlation between the intercept and light extinction. There was a trend towards a positive correlation but it was not statistically significant (P=0.200).

DISCUSSION

The highly significant linear relationship we obtained between DSM and DEM for all sites (excluding August data) is promising (**Eq. 4**; **Figure 9b**), even though there is a great deal of unexplained variation. Much of this is related to wetland-specific conditions that may make it undesirable to develop a single predictive equation for all wetlands because of all the factors that would need to be included in the model. One reason for the difference between Green Island and North Bay 1 is the colour of the water. North Bay 1 is a protected wetland that receives high organic carbon, making the water highly coloured. Its location within North Bay also makes it unlikely to be diluted by open waters of Georgian Bay. The overestimates of depth may be due to its dystrophic condition. By contrast, Green Island is most exposed to open waters of Georgian Bay and consequently has very low organic carbon content that do not interfere with light penetration. This may explain why the DSM were underestimates of DEM, especially when the colour of the sandy substrate was also light-coloured. To fully test this, we would need data from more sites than we have in our existing database. Water colour is not a parameter that is collected routinely but may be added in future surveys.

Different habitat classes and spatial features can greatly affect the DSM depth accuracy. Although we expected that imperfect rendering would yield the highest inaccuracies and clear water would the lowest, these effects were inconsistent across wetlands. For example, presence of aquatic vegetation resulted in some of the most accurate DSM values for Green Island while they led to some of the least accurate values for Venning's Bay. Therefore, this study failed to identify consistent effects of microhabitat class and spatial features on depth accuracies. We do not know the reason for the discrepancies associated with the clear water class, but we noted that there was a negative relationship between light penetration and the level of discrepancies (i.e. greater light penetration for Green Island and least for North Bay; see Table 1; perfect Spearman's rank correlation not shown).

Some discrepancies between DEM and DSM estimates are undoubtedly related to inaccuracies of the DEM, both with respect to inaccurate sonar readings at depths shallower than 0.7 m, and the coarseness of Weller and Chow-Fraser's (2019) 10-m DEM that we used for the three wetlands. Another factor is that acquisition of drone image and sonar data were at different times for different projects. Future field studies should ensure that both sets of data are acquired simultaneously (at the same water level and water clarity/ colour conditions) and that dGPS data are collected to serve as ground-control points to produce accurate elevations and shoreline so that we can properly scale the DSM information and link them to actual depths rather than relative depths.

We do not know why the DSM data for August in both the North Bay 1 and Venning's Bay wetlands were problematic. One possible reason may not be due to the timing but differences in water levels on the days of the surveys. Water-level interacts with the wetland bathymetry and can influence the ease with which the sonar data are acquired, and the amount of emergent and floating vegetation that may interfere with accuracies of the DSM. In general, though, it makes sense to acquire images in wetlands before the cover of aquatic vegetation reach their prime, and before the plants make it difficult for a boat to navigate in the shallow portions of the wetland. Therefore, we recommend that the field work be carried out in June and July if possible.

The correlation between intercepts of the wetland-specific regressions between DSM and DEM and light extinction was not statistically significant, but there was a general trend towards higher intercepts when light penetration was more limited. This is consistent with the hypothesis that the dystrophic nature of wetlands with high extinction coefficients leads to overestimates of depths. More data should be collected to rigorously test this hypothesis. We also found a highly significant negative relationship between discrepancies in "clear water" habitat class and light extinction coefficient; we cannot provide an explanation for this but recommend that more effort be spent to determine if this is spurious or real.

The maximum depth associated with wetland DEMs in this study did not exceed 2.5 m. Hence, these data are not suitable for determining depth limitations for applying our relationships between DSM and DEM.

CONCLUSION AND RECOMMENDATION

Given that we only had four wetlands in this study and that data had not been collected specifically for this study, our results show that DSM could be a good alternative to sonar technology for providing bathymetric data. Future steps should be taken to apply the equations to wetlands to generate bathymetric information to develop a drone-DEM for comparison with the sonar-DEM. A proper study should be developed to ensure that sonar and drone acquisitions are simultaneous and that ground control points are also collected at the same time with dGPS along the shoreline.

ACKNOWLEDGEMENTS

We wish to acknowledge past contributions from graduate students who collected data that we are using in this project. Drone operators in the past have included James Marcaccio, Nick Luymes, Stuart Campbell and Gillian Chow-Fraser. Bathymetric information have been collected by many students but especially Dan Weller and Lindsey Boyd. This report was supported in part by a contract from Fisheries and Oceans Canada.

LITERATURE CITED

Arseni, M., Voiculescu, M., Georgescu, L. P., Iticescu, C., & Rosu, A. (2019). Testing Different Interpolation Methods Based on Single Beam Echosounder River Surveying. Case Study: Siret River. *ISPRS International Journal of Geo-Information, 8*(11), 507. doi:10.3390/ijgi8110507

Lind, Owen T. 1985. Handbook of common methods in Limnology. Kendall/Hunt Publishing Company. 2nd Edition.

Marcaccio, J.V., Markle, C.E. and Chow-Fraser, P. 2016. Use of fixed-wing and multi-rotor unmanned aerial vehicles to map dynamic changes in a freshwater marsh. J. Unmanned Veh. Syst. 4: 193-202.

Mazzoleni, M., Paron, P., Reali, A., Juizo, D., Manane, J., & Brandimarte, L. (2020). Testing UAV-derived topography for hydraulic modelling in a tropical environment. *Natural Hazards, 103*(1), 139-163. doi:10.1007/s11069-020-03963-4

Monteiro, J. G., Jiménez, J. L., Gizzi, F., Přikryl, P., Lefcheck, J. S., Santos, R. S., & Canning-Clode, J. (2021). Novel approach to enhance coastal habitat and biotope mapping with drone aerial imagery analysis. *Scientific Reports, 11*(1). doi:10.1038/s41598-020-80612-7

Paul, J. D., Buytaert, W., & Sah, N. (2020). A Technical Evaluation of Lidar-Based Measurement of River Water Levels. *Water Resources Research, 56*(4). doi:10.1029/2019wr026810

Pegau, W. S., Gray, D., & Zaneveld, J. R. (1997). Absorption and attenuation of visible and near-infrared light in water: Dependence on temperature and salinity. *Applied Optics, 36*(24), 6035. doi:10.1364/ao.36.006035

Pillay, T., Cawthra, H., & Lombard, A. (2020). Characterisation of seafloor substrate using advanced processing of multibeam bathymetry, backscatter, and sidescan sonar in Table Bay, South Africa. *Marine Geology, 429*, 106332. doi:10.1016/j.margeo.2020.106332

US Department of Commerce, N. O. (2012, October 01). What is LIDAR. Retrieved from https://oceanservice.noaa.gov/facts/lidar.html#:~:text=Two types of lidar are,measure seafloor and riverbed elevations

Weller, J.D. and Chow-Fraser, P. 2019. 2019. Hydrogeomorphic modeling of low-marsh habitat in coastal Georgian Bay, Lake Huron. Wetlands Ecology and Management. 27: 207-221.

Table 1: Details on timing of image acquisitions by UAV, depth information collected by sonar, and associated water levels for the four wetlands in this study. Date format is mm-dd-yyyy. Bolded numbers are those that were used in this study.

Wetland	UAV acquisition		Sonar acquisition	Light extinction	
	Date	**Water level**	**Date**	**Date**	**Value**
Green Island	06-06-2016 07-25-2017	176.715 176.897	06-10-2016, 08-25-2016, 08-30-2016, 07-25-2017,	06-02-2004 **07-09-2015** **08-24-2016**	1.778 **1.142** **1.372**
North Bay 1	08-18-2016 06-14-2017	176.751 176.708	09-21-2009, 08-10-2009, 08-11-2009, 08-24-2016	06-15-2005 **08-18-2016**	2.042 **2.266**
Ojibway Bay	07-19-2016	176.793	08-19,2016	06-14-2005 **08-15-2016**	1.262 **1.346**
Venning's Bay	06-03-2015 08-24-2015	176.526 176.793	06-29-2020, 07-02-2020	**05-26-2010**	**1.748**

Table 2. Comparison of scaled elevation values acquired with dGPS and derived from DSM for the North Bay 1 wetland. Data were acquired on August 18, 2016. Values were scaled by subtracting minimum dGPS or DSM values from individual locations and dividing the resulting values by the maximum so that we would have corresponding values between 0 and 100.

Latitude	Longitude	dGPS	DSM	Scaled dGPS	Scaled DSM
44.899509	-79.794503	178.33636	-66.429634	0.000	0.000
44.899521	-79.794542	179.26836	-65.85556	0.245	0.129
44.899454	-79.79462	179.48536	-65.740334	0.302	0.155
44.899851	-79.794497	180.86436	-63.708252	0.664	0.611
44.899512	-79.794653	181.33636	-64.079803	0.788	0.528
44.899567	-79.794617	181.60536	-63.067818	0.859	0.755
44.899663	-79.794542	181.91436	-62.750301	0.940	0.826
44.899589	-79.794679	182.14236	-61.977791	1.000	1.000

Figure 1: Location of the 4 wetlands in southeastern Georgian Bay.

Figure 2. Mosaic of UAV images acquired in North Bay 1 wetland on August 18, 2016. a) Closeup of the 8 dGPS points taken above the water. b) Overview of entire wetland showing the glare on the water.

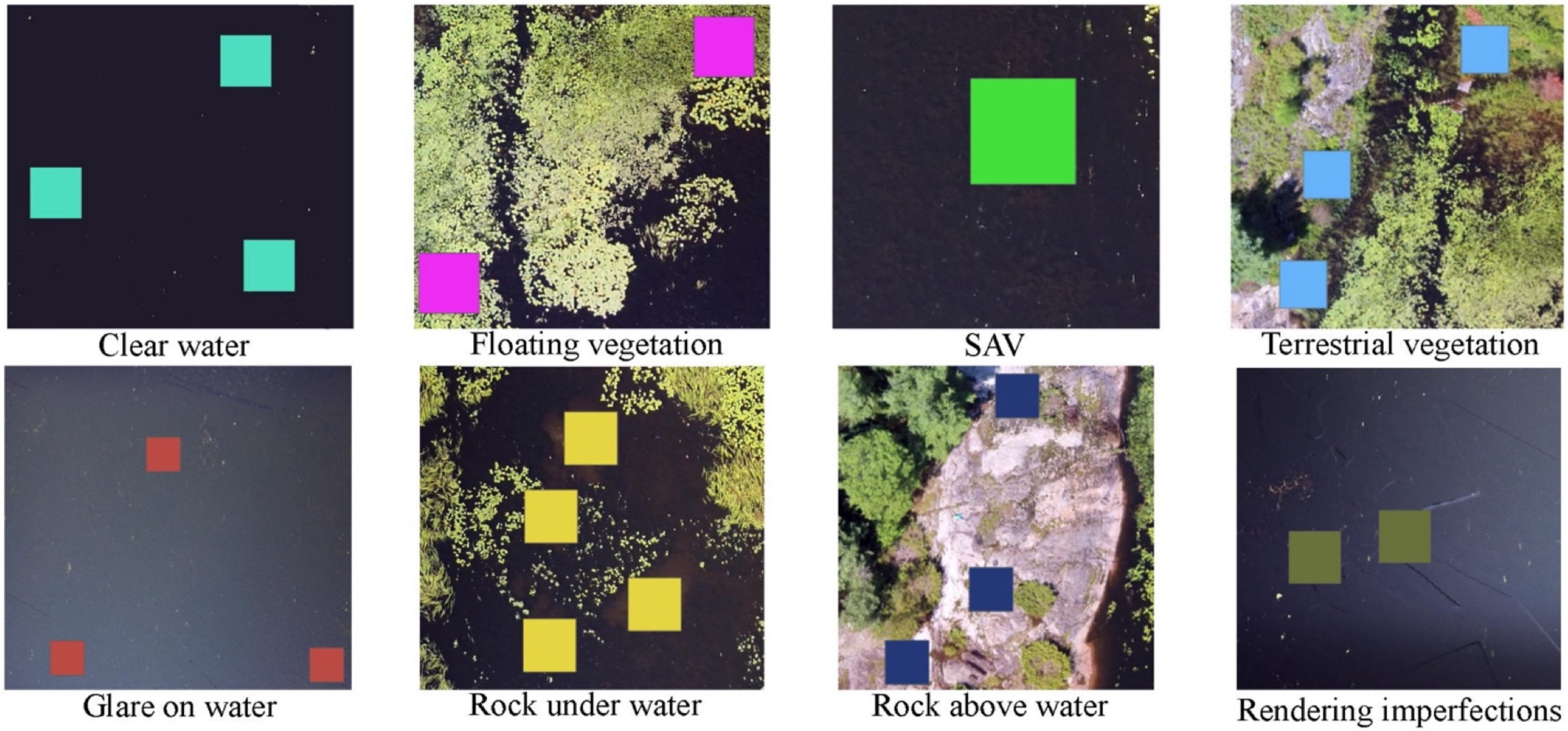

Figure 3. Classes of habitat features or groups used for North Bay 1 wetland of the orthophoto taken on August 18, 2016. Coloured blocks are the difference spatial features and where it covers the orthophoto/DSM.

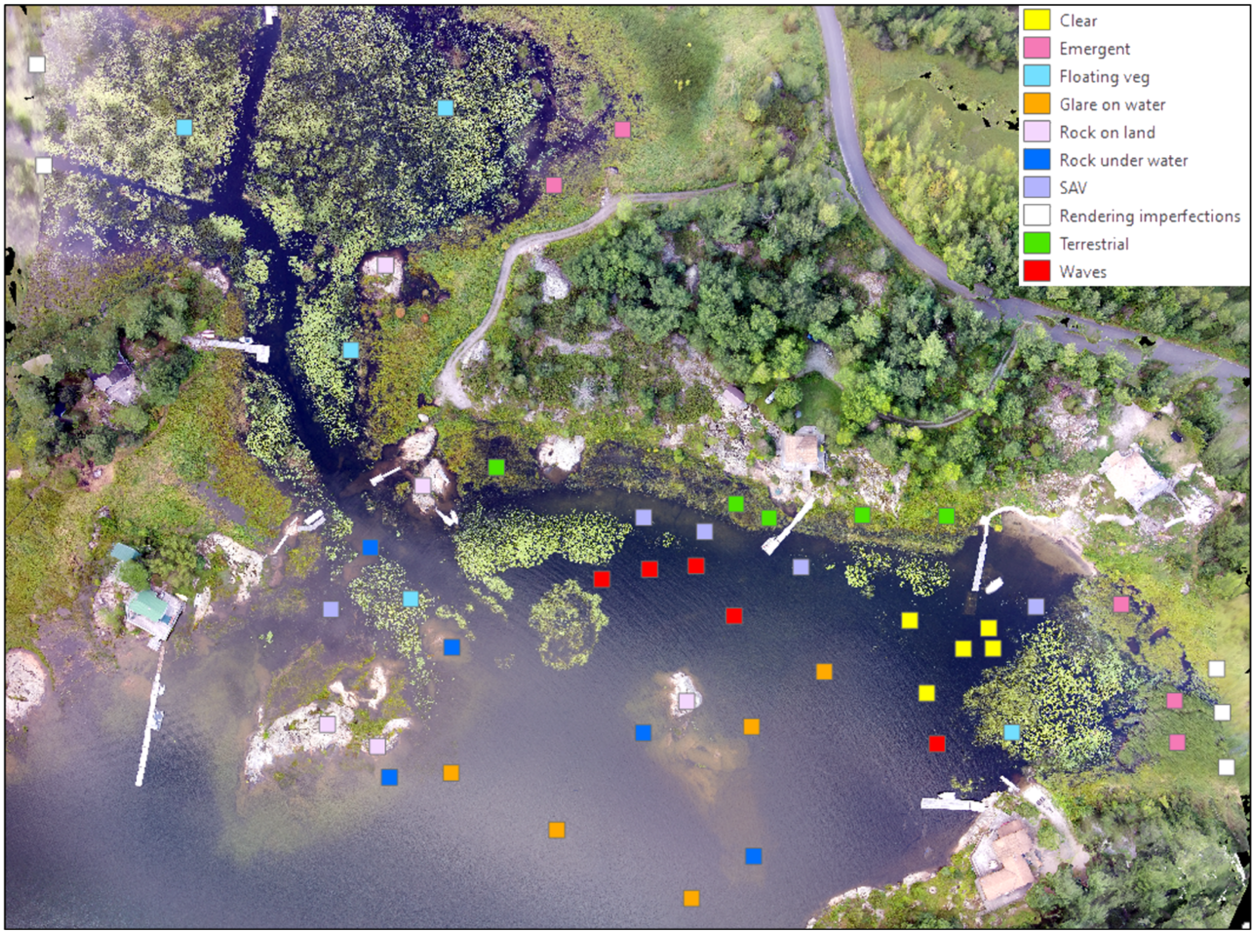

Figure 4: Drone image of the Venning's Bay wetland with placement of quadrats (25 m^2) used to determine the potential effect of microhabitat classes and spatial features on accuracy of depth estimates.

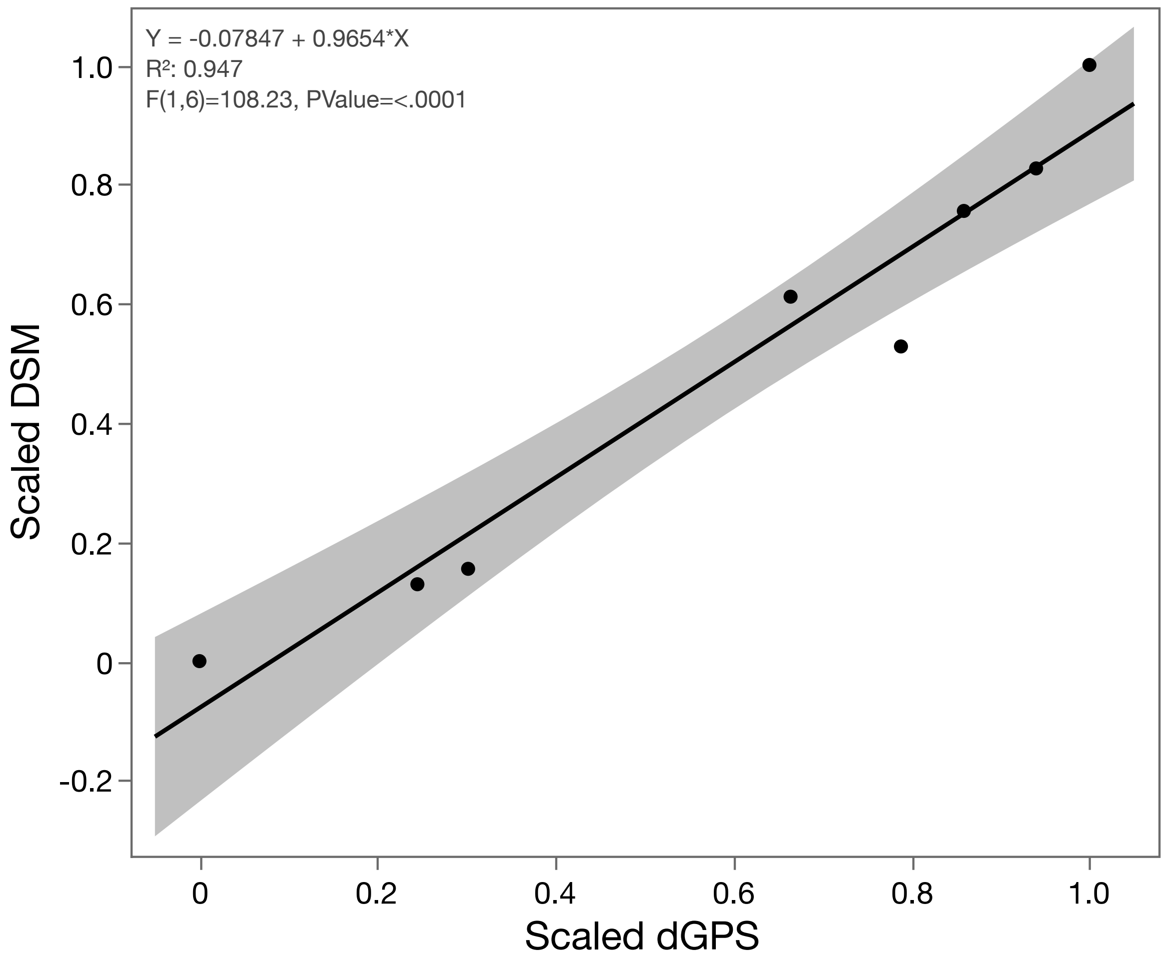

Figure 5: Elevation data corresponding to a digital surface model (DSM) derived from UAV images versus elevation data acquired a dGPS for North Bay 1 wetland. (See raw data in Table 1).

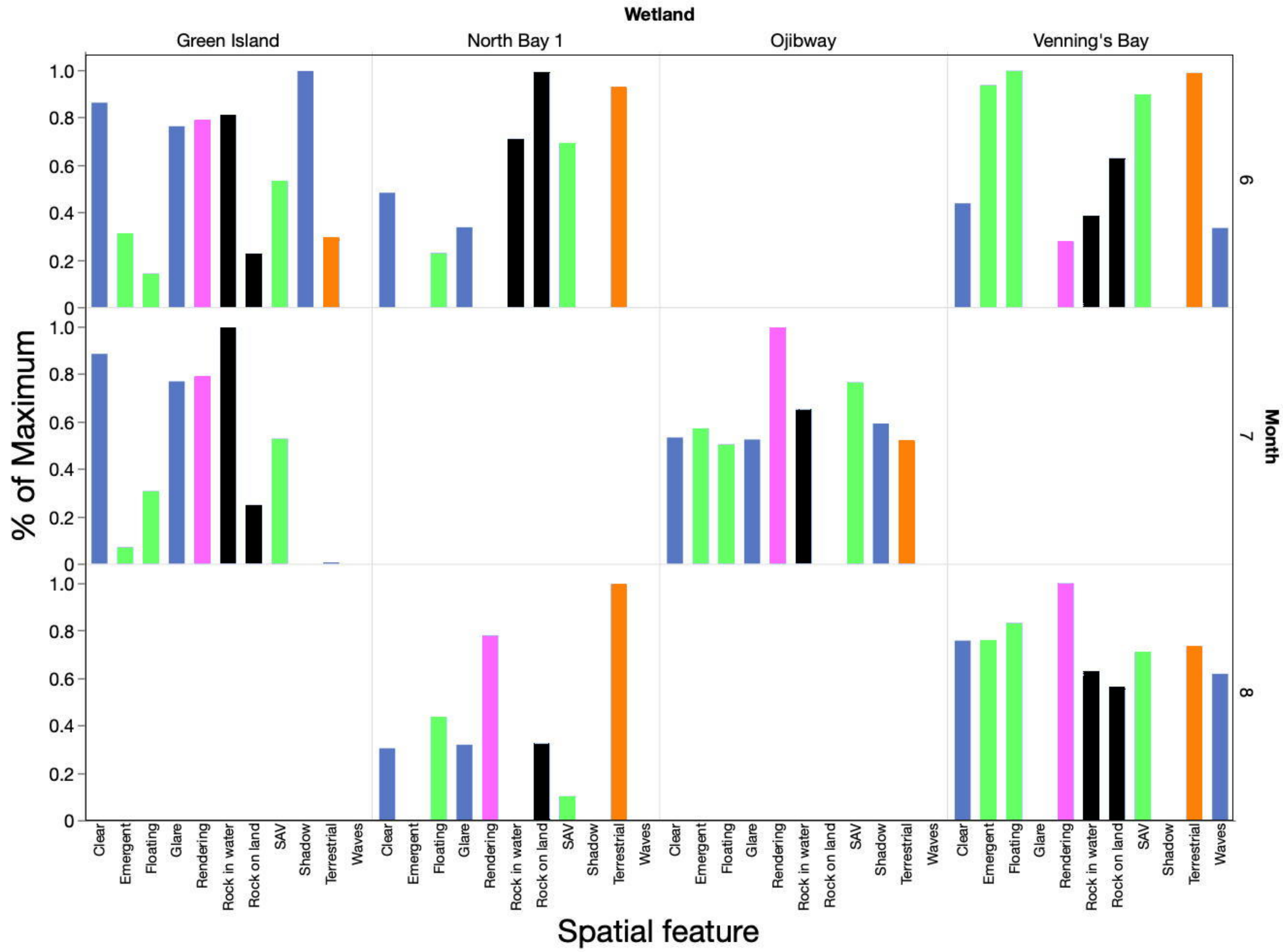

Figure 6: Depth values obtained by DEM subtracting depth values for DSM expressed as a percentage of highest differences. Blue bars correspond to water; green bars correspond to aquatic vegetation; purple correspond to rendering imperfections; black bars correspond to rocks; organge bars correspond to terrestrial vegetation.

a)

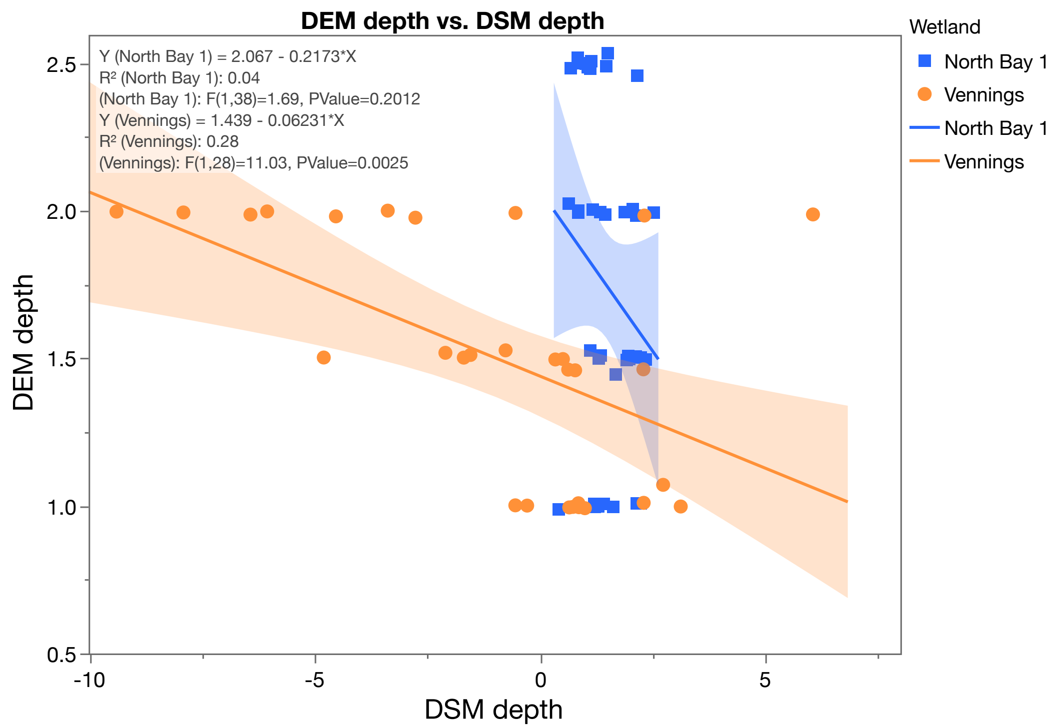

b)

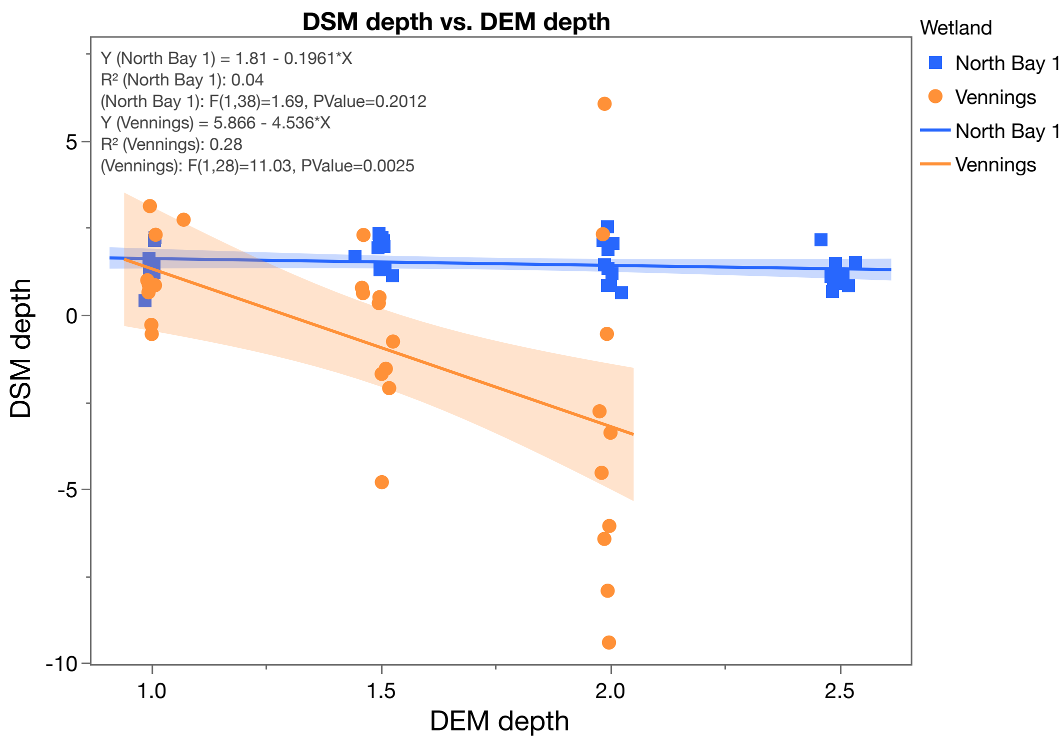

Figure 7: Regression analysis for North Bay 1 and Venning's Bay wetlands during August. a) DEM regressed against DSM and b) DSM regressed against DEM.

a)

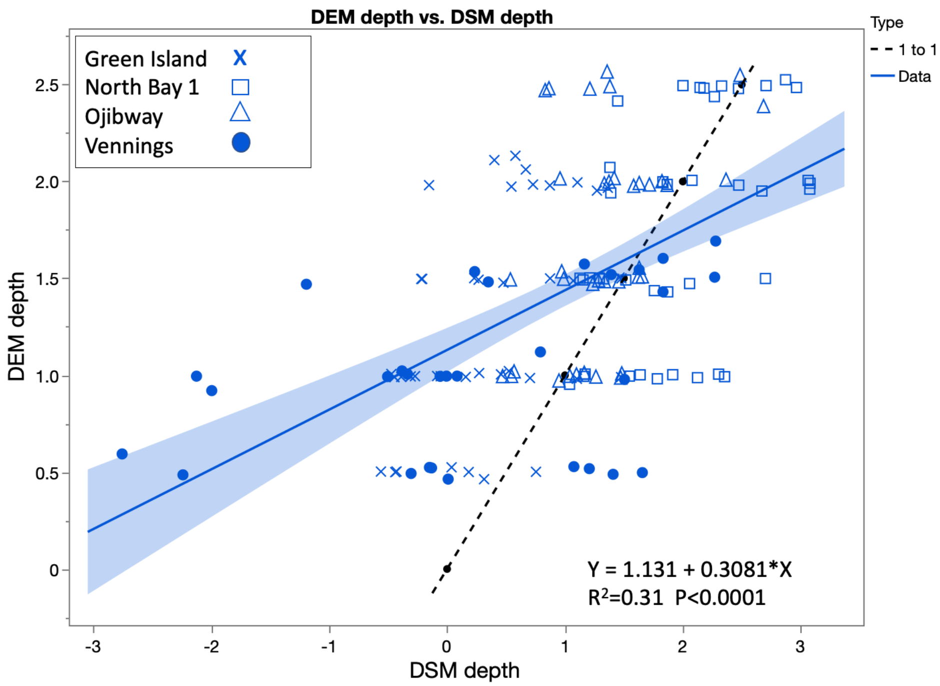

b)

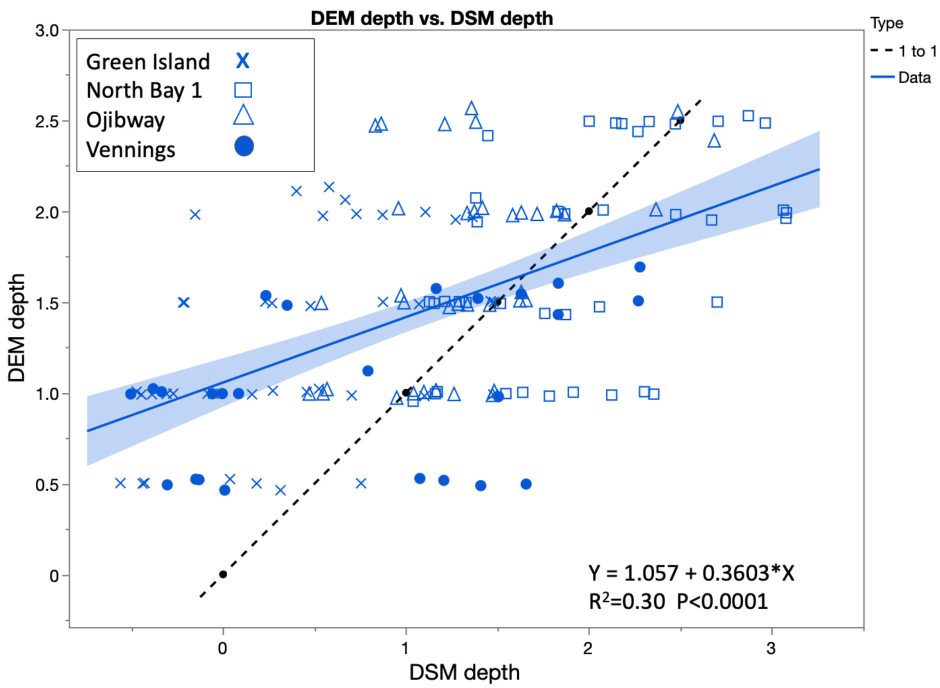

Figure 8: Regression of DEM against DSM when a) all June and July data were considered and b) when low DSM values from Venning's Bay were excluded from dataset. Dotted line is when DEM=DSM.

a)

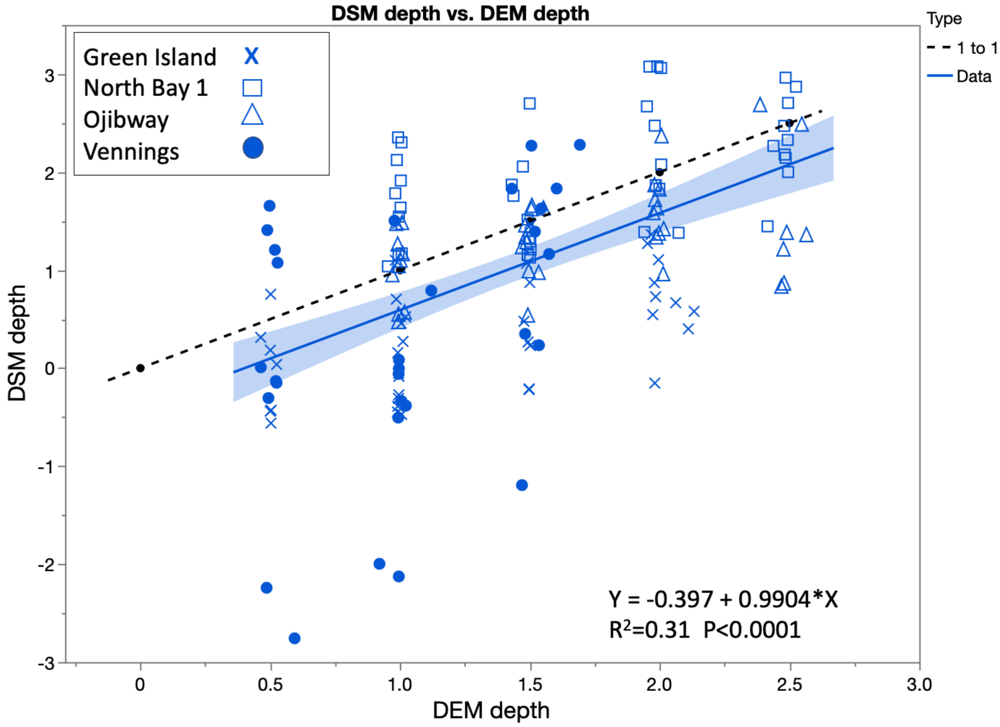

b)

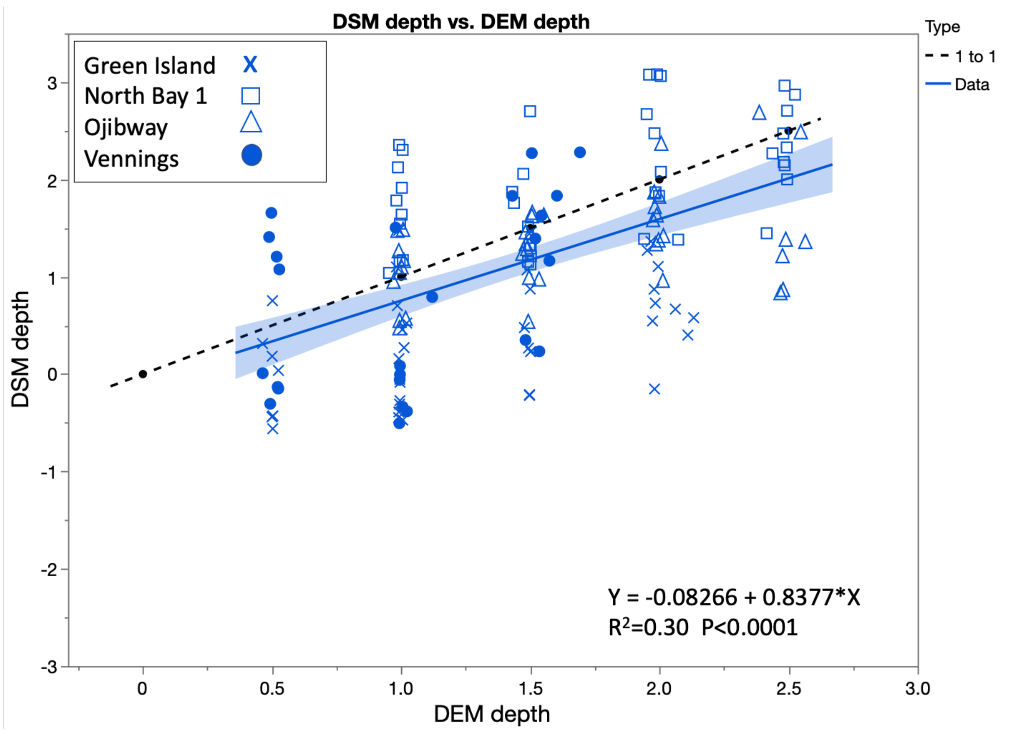

Figure 9: Regression of DSM against DEM when a) all data in June and July were considered and b) when low DSM values from Venning's Bay were excluded. Dotted line is when DSM=DEM.

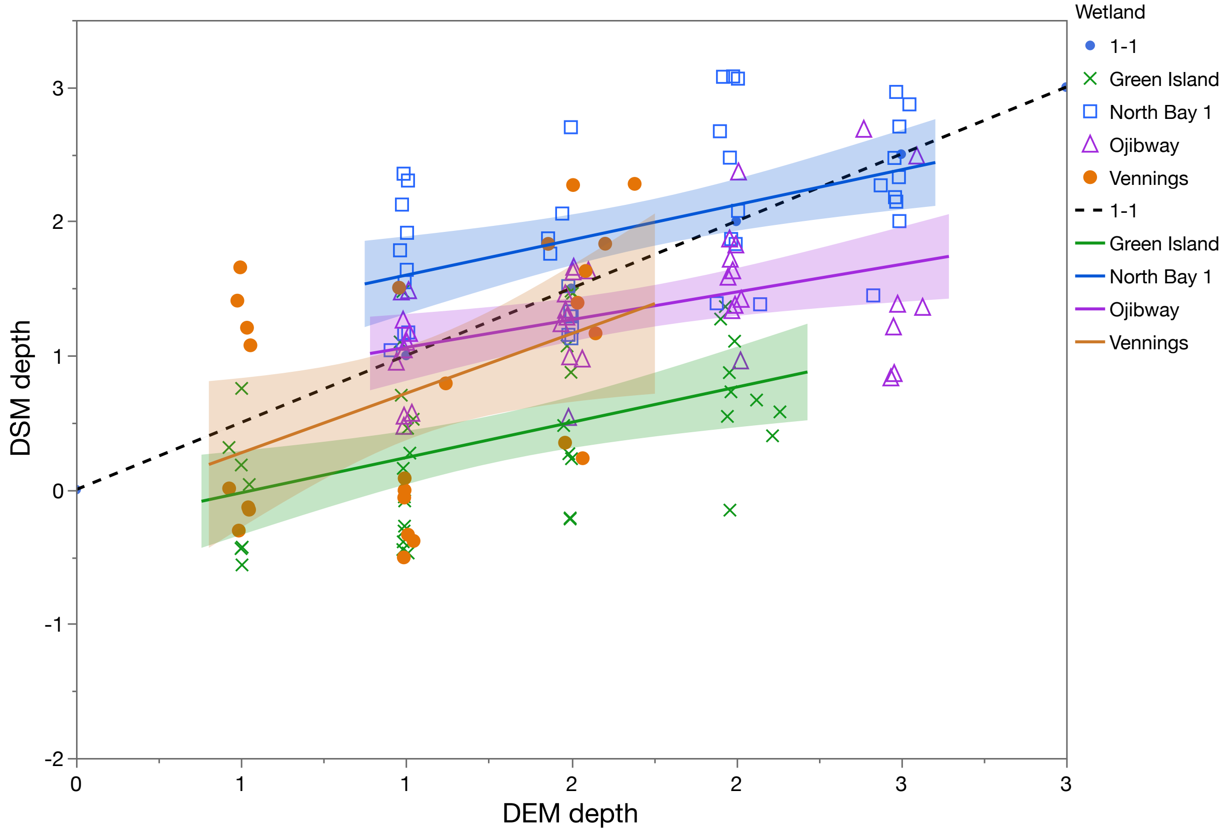

Figure 10: Linear regression analysis of DSM against DEM performed separately for each wetland for June and July data only. Dotted line is when DSM=DEM.

APPENDICES

DSM and DEM maps and UAV images for all wetland-years in this study.

Figure A1: a) DSM created by Pix4D Mapper from UAV images acquired on June 3, 2015 and b) DEM created by interpolation of depth information acquired by sonar on Venning's Bay).

Figure A2: a) DSM created by Pix4D Mapper from UAV images acquired on August 24, 2015 and b) DEM created by interpolation of depth information acquired by sonar in Venning's Bay.

Figure A3: Mosaic of UAV images of Venning's Bay acquired on a) June 3, 2015 and b) August 24, 2015. Water levels on June 3 and August 24 were 176.526 m and 176.793 m, respectively, a difference of 26.7 cm.

Figure A4: a) DSM created by Pix4D Mapper from UAV images acquired on July 19, 2016 in Ojibway Bay. b) DEM created by interpolation of depth information acquired by sonar. c) Mosaic of UAV images, showing location of quadrats (25 m^2) strategically sampled for direct comparison of depths calculated from DSM and DEM.

Figure A5: a) DSM created by Pix4D Mapper from UAV images acquired on August 18, 2016 in North Bay 1. b) DEM created by interpolation of depth information acquired by sonar. c) Mosaic of UAV images, showing location of quadrats (25 m^2) strategically sampled for direct comparison of depths calculated from DSM and DEM.

Figure A6: a) DSM created by Pix4D Mapper from UAV images acquired on June 14, 2017 in North Bay 1. b) DEM created by interpolation of depth information acquired by sonar. c) Mosaic of UAV images, showing location of quadrats (25m^2) strategically sampled for direct comparison of depths calculated from DSM and DEM.

Figure A7: a) DSM created by Pix4D Mapper from UAV images acquired on June 16, 2016 in Green Island wetland. b) DEM created by interpolation of depth information acquired by sonar. c) Mosaic of UAV images, showing location of quadrats (25 m^2) strategically sampled for direct comparison of depths calculated from DSM and DEM

Table A1: Differences between depths obtained from DSM and DEM for North Bay 1 Wetland on June 14, 2017.

Table A2: Differences between depths obtained DSM vs DEM for all wetlands (see Table 1 for relevant dates).

a)

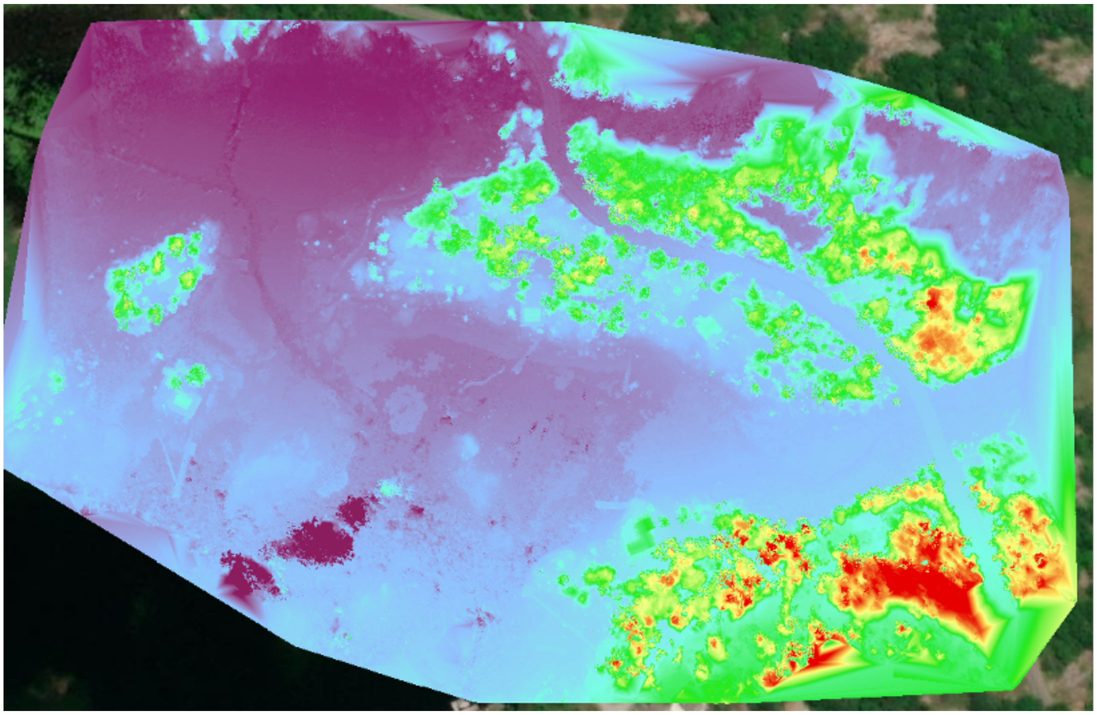

b)

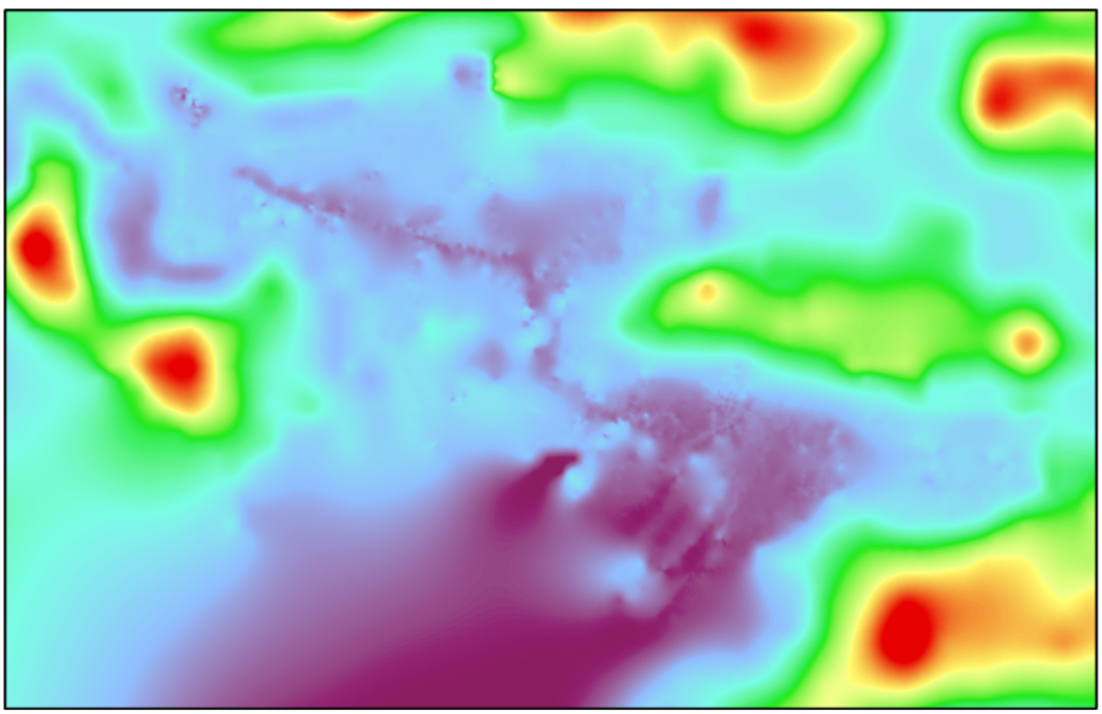

Figure A1: a) DSM created by Pix4D Mapper from UAV images acquired on June 3, 2015 and b) DEM created by interpolation of depth information acquired by sonar on Venning's Bay).

a)

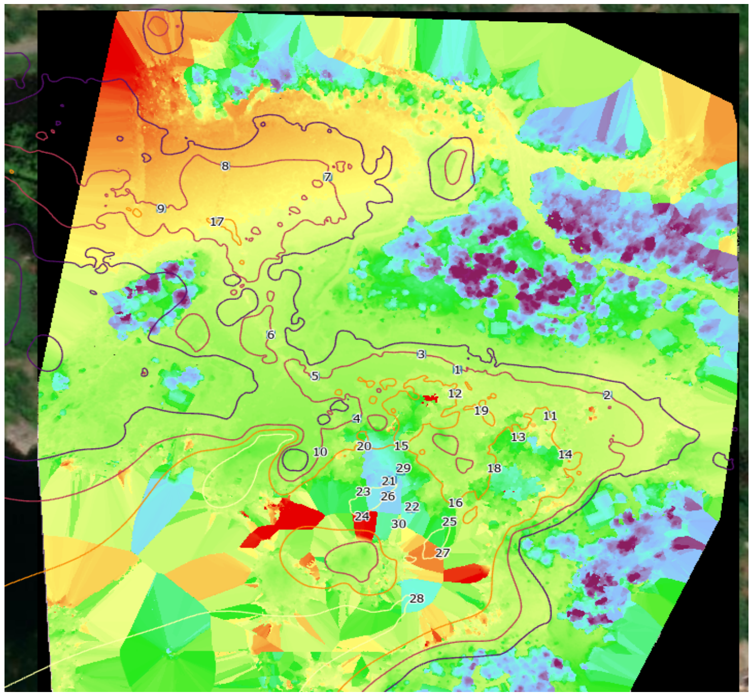

b)

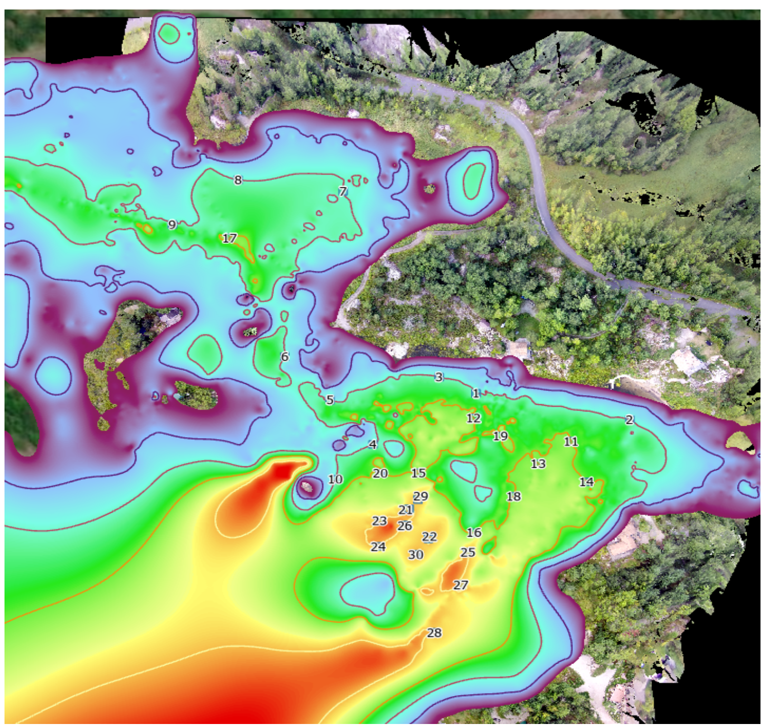

Figure A2: a) DSM created by Pix4D Mapper from UAV images acquired on August 24, 2015 and b) DEM created by interpolation of depth information acquired by sonar in Venning's Bay.

a)

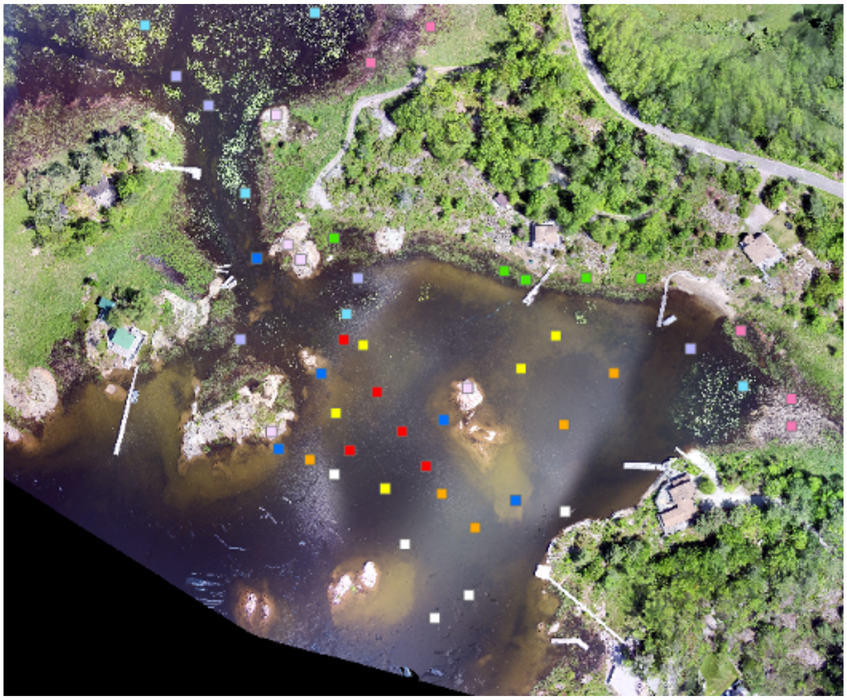

b)

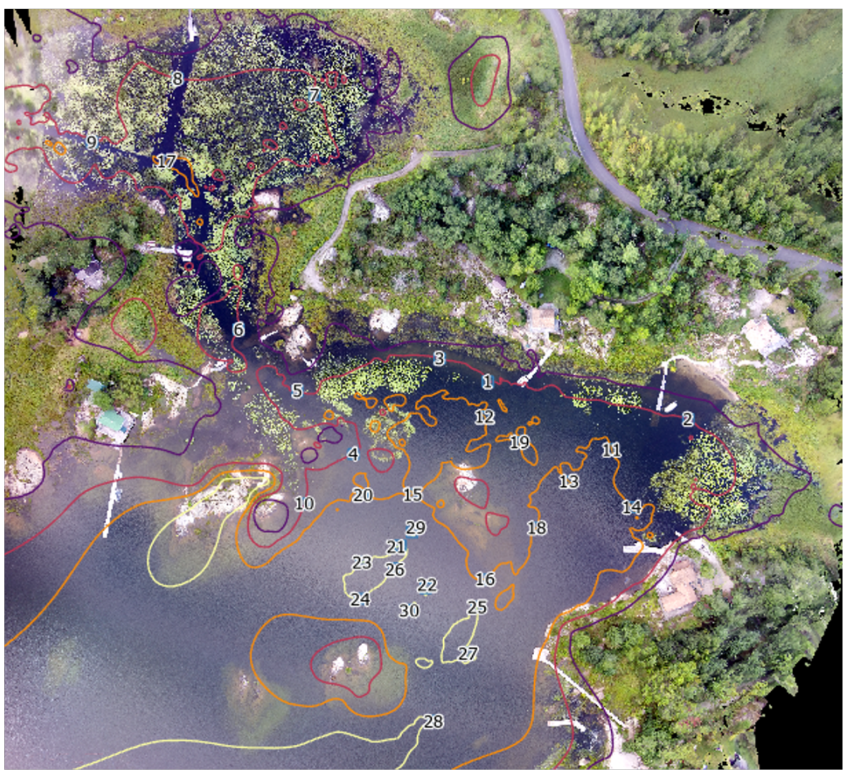

Figure A3: Mosaic of UAV images of Venning's Bay acquired on a) June 3, 2015 and b) August 24, 2015. Water levels on June 3 and August 24 were 176.526 m and 176.793 m, respectively, a difference of 26.7 cm.

a)

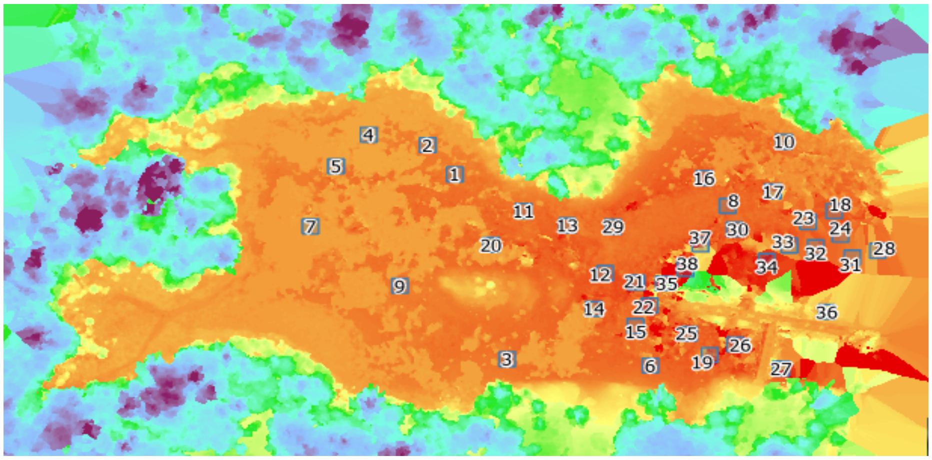

b)

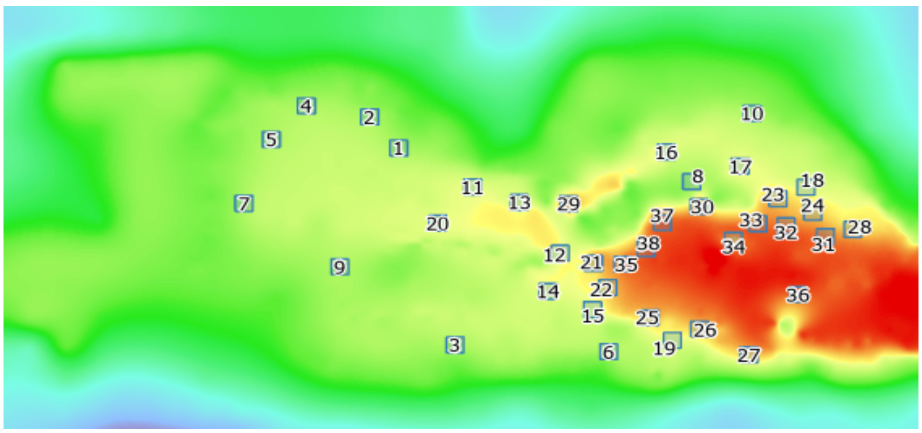

b)

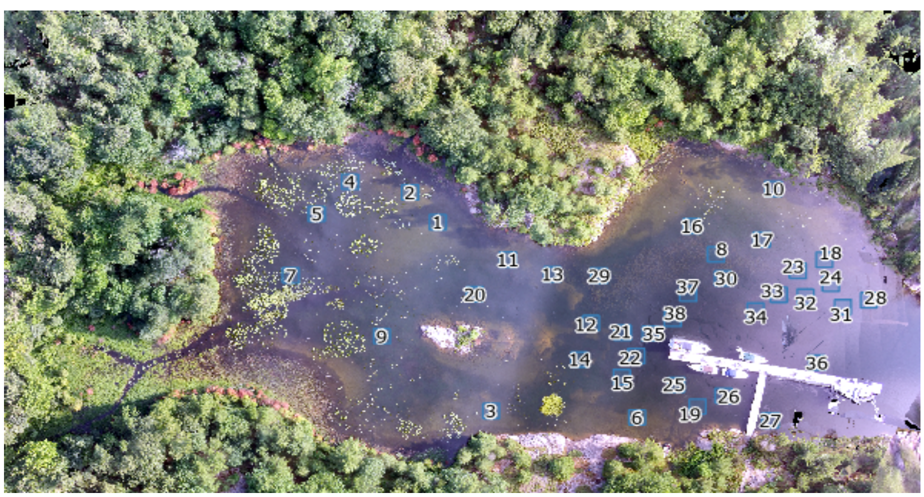

Figure A4: a) DSM created by Pix4D Mapper from UAV images acquired on July 19, 2016 in Ojibway Bay. b) DEM created by interpolation of depth information acquired by sonar. c) Mosaic of UAV images, showing location of quadrats (25 m^2) strategically sampled for direct comparison of depths calculated from DSM and DEM.

a) b) c)

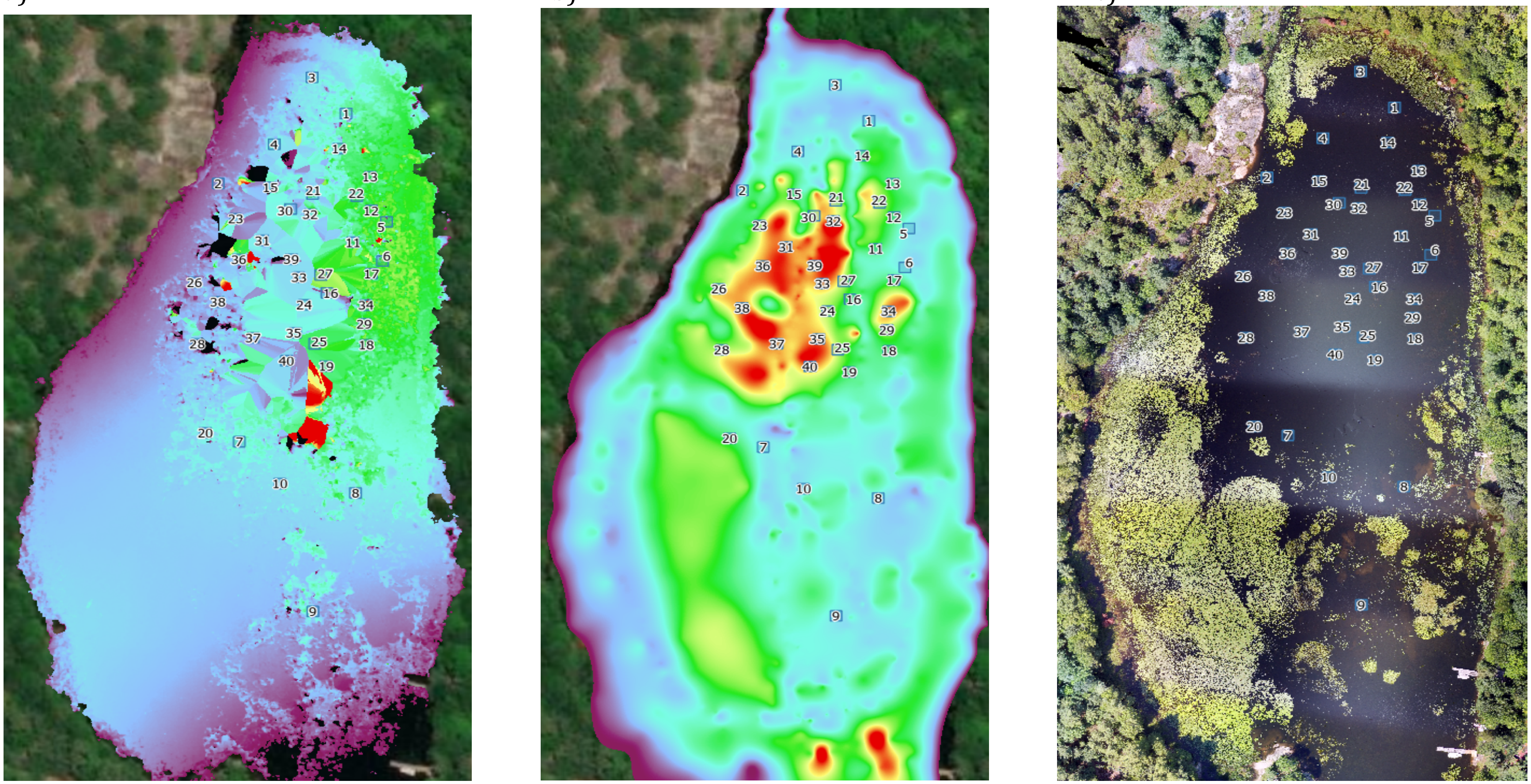

Figure A5: a) DSM created by Pix4D Mapper from UAV images acquired on August 18, 2016 in North Bay 1. b) DEM created by interpolation of depth information acquired by sonar. c) Mosaic of UAV images, showing location of quadrats (25 m^2) strategically sampled for direct comparison of depths calculated from DSM and DEM.

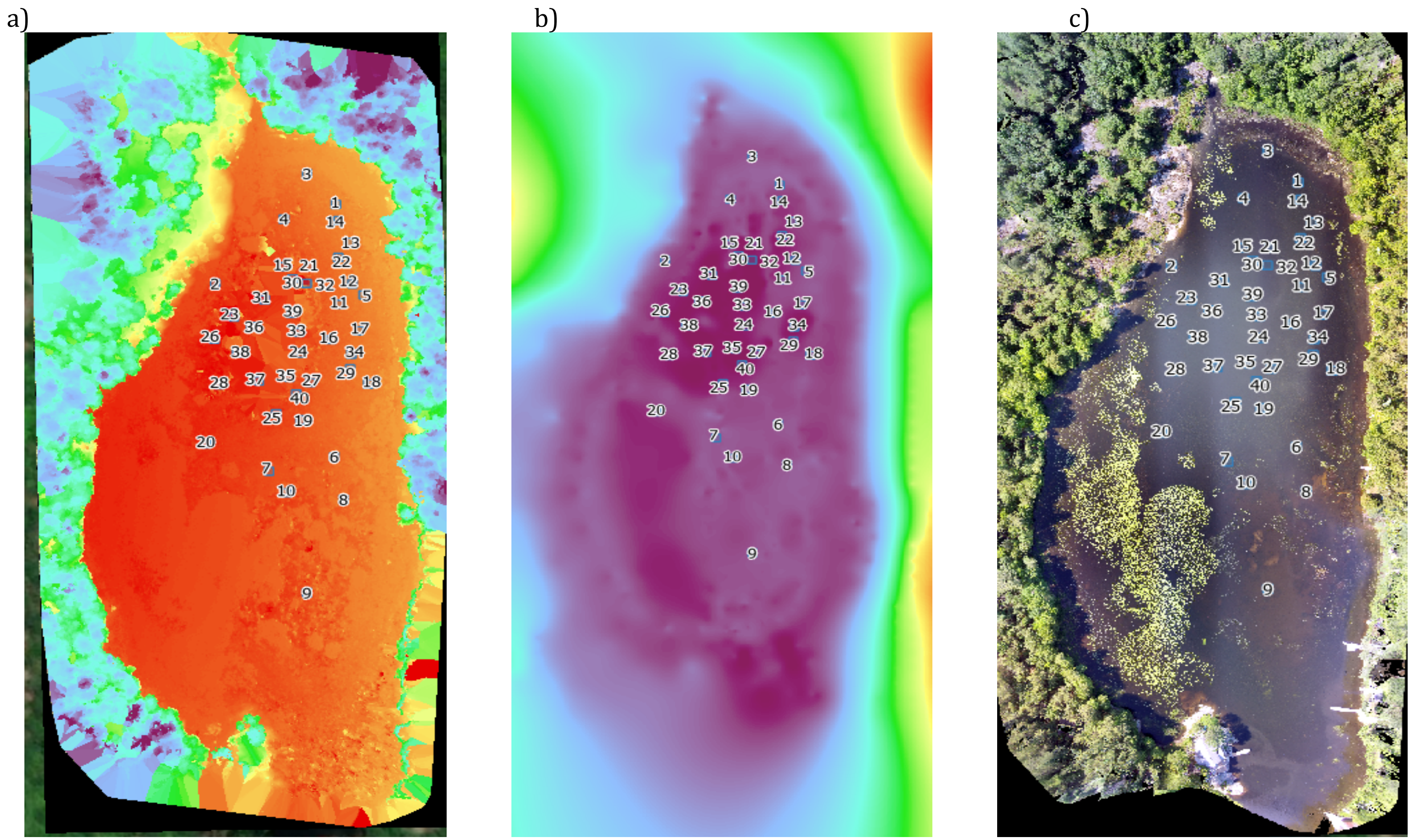

Figure A6: a) DSM created by Pix4D Mapper from UAV images acquired on June 14, 2017 in North Bay 1. b) DEM created by interpolation of depth information acquired by sonar. c) Mosaic of UAV images, showing location of quadrats ($25m^2$) strategically sampled for direct comparison of depths calculated from DSM and DEM.

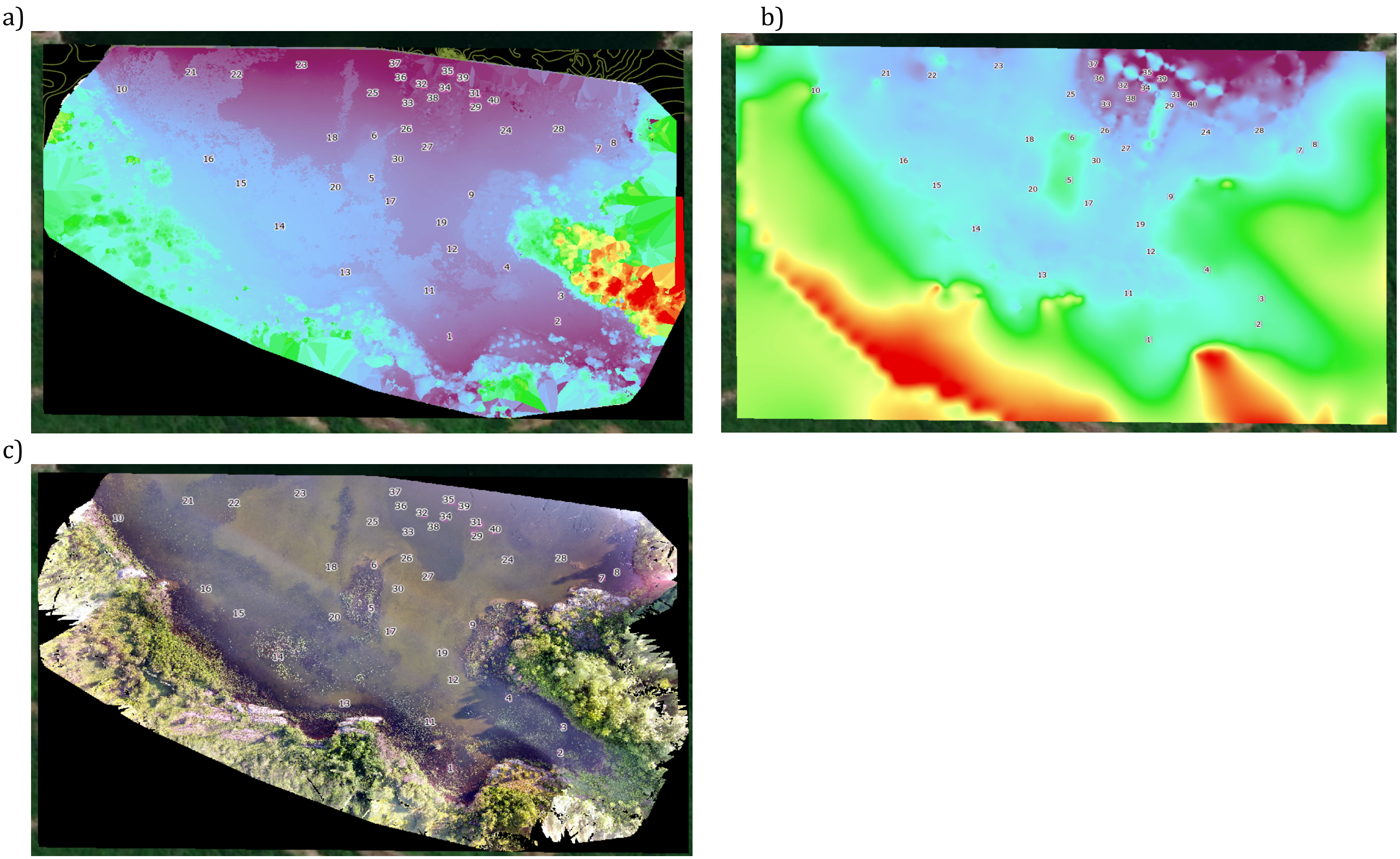

Figure A7: a) DSM created by Pix4D Mapper from UAV images acquired on June 16, 2016 in Green Island wetland. b) DEM created by interpolation of depth information acquired by sonar. c) Mosaic of UAV images, showing location of quadrats (25 m^2) strategically sampled for direct comparison of depths calculated from DSM and DEM.

Table A1: Differences between depths obtained from DSM and DEM for North Bay 1 Wetland on June 14, 2017. Min, Max, Range and Mean refer to the minimum, maximum, range and mean of all DSM values within each quadrat (25 m^2) located in 8 class/features. Overall mean and range refer to the mean of all values within the class/feature. Mean of the range refers to the average range within cells for the class/feature.

Class/Feature	Min	Max	Range	Mean	Overall mean	Overall range	Mean of range
Clear water	-4.08	-1.55	2.53	-2.82	-2.55	0.42	1.66
	-3.00	-1.52	1.48	-2.40			
	-3.69	-1.86	1.83	-2.48			
	-3.29	-1.57	1.72	-2.52			
	-2.84	-2.10	0.75	-2.55			
Floating vegetation	-2.55	-2.27	0.28	-2.42	-2.29	1.42	0.41
	-2.69	-2.40	0.29	-2.55			
	-1.63	-1.28	0.35	-1.47			
	-2.42	-1.77	0.66	-2.13			
	-3.09	-2.61	0.48	-2.89			
SAV	-4.11	-3.47	0.64	-3.79	-2.95	2.09	0.80
	-3.62	-2.79	0.82	-3.16			
	-3.48	-2.46	1.02	-2.90			
	-2.44	-1.32	1.12	-1.70			
	-3.39	-2.97	0.42	-3.17			
Terrestrial plants	-1.57	-0.66	0.90	-1.25	-1.18	2.12	0.90
	-1.34	0.23	1.57	-1.04			
	-0.53	0.21	0.74	-0.28			
	-2.93	-2.09	0.85	-2.40			
	-1.10	-0.67	0.44	-0.93			
Glare	-3.03	-2.50	0.53	-2.82	-2.52	0.49	0.87
	-2.61	-1.98	0.63	-2.33			
	-2.91	-2.11	0.81	-2.39			
	-3.86	-2.17	1.69	-2.53			
	-3.01	-2.29	0.71	-2.55			
Rock under water	-3.39	-2.80	0.59	-3.20	-3.15	1.25	0.63
	-4.21	-3.17	1.04	-3.56			
	-3.61	-3.32	0.28	-3.47			
	-2.77	-1.90	0.87	-2.31			
	-3.43	-3.04	0.38	-3.23			
Rock above water	-5.14	-2.62	2.52	-3.40	-2.51	2.92	4.13
	-5.59	-0.30	5.29	-0.66			
	-5.49	1.28	6.77	-3.58			
	-3.44	0.99	4.44	-1.95			
	-3.75	-2.14	1.61	-2.96			
Rendering imperfections	-3.01	-2.26	0.75	-2.69	-1.61	2.14	1.42
	-3.04	-2.48	0.56	-2.68			
	-1.95	0.07	2.02	-0.54			
	-1.43	0.32	1.76	-0.71			
	-2.46	-0.46	2.00	-1.40			

Table A2: Differences between depths obtained DSM vs DEM for all wetlands (see Table 1 for relevant dates). Overall mean refers to the mean of all values within the class/ feature. Overall mean and range refer to the mean of all values within the class/feature. Mean of the range refers to the average range within cells for the class/feature. Clear=clear water; EV=Emergent vegetation; FV=Floating vegetation; Glare=Glare on water; RUW=Rocks under water; RAW=Rocks above water; RI=Rendering imperfections; SAV=Submersed aquatic vegetation; SHAD=Shadow; TV=Terrestrial vegetation); WV=Waves.

	North Bay 1 (2016)			**Ojibway Bay**			**Green Island (2017)**			**Green Island (2016)**			**Venning's Bay (Aug)**			**Venning's Bay (June)**		
Class/ feature	Overall Mean	Overall Range	Mean of range	Overall Mean	Overall Range	Mean of range	Overall Mean	Overall Range	Mean of range	Overall Mean	Overall Range	Mean of range	Overall Mean	Overall Range	Mean of range	Overall Mean	Overall Range	Mean of range
Clear	-1.36	2.52	5.10	244.28	0.59	1.75	206.58	0.62	1.21	214.58	0.96	0.57	260.68	1.55	3.64	249.07	2.12	2.44
EV				244.37	0.45	0.35	205.03	1.27	1.10	213.86	1.98	0.47	260.69	2.51	1.13	250.22	4.49	1.02
FV	-1.64	0.40	0.29	244.21	0.64	0.29	205.48	0.46	0.66	212.71	1.40	0.27	261.08	3.20	0.33	250.36	3.69	0.78
Glare	-1.52	1.10	1.44	244.26	0.73	1.89	206.36	1.33	0.70	214.39	2.77	0.73	256.57	8.87	1.88	248.06	2.09	3.31
RI	-1.89	5.10	9.34	245.38	5.94	7.61	206.40	1.43	1.11	214.46	0.95	1.36	261.99	3.55	0.54	248.70	10.32	6.08
RIW	-0.80	3.06	9.44	243.02	1.59	1.73	205.37	1.22	1.81	213.17	1.57	1.18	259.62	3.74	0.74	249.51	3.58	0.93
RAW	-1.11	1.05	0.94	244.56	1.12	0.85	206.79	1.22	1.01	214.16	2.17	1.04	259.98	0.64	1.27	248.95	2.93	1.99
SAV	-1.13	0.55	0.20	244.83	0.81	0.90	205.90	1.12	1.75	213.90	2.20	1.37	260.42	1.21	0.59	250.13	1.88	1.15
SHAD				244.42	0.54	1.37				214.76	1.76	0.93						
TV	-0.87	4.96	11.88	244.25	0.48	4.10	204.91	2.16	3.30	213.91	4.49	3.17	260.55	1.07	0.51	250.34	0.35	1.45
WV													259.92	0.25	1.40	248.83	1.35	3.06